



## Evidence for a Magnetic Proximity Effect up to Room Temperature at Fe/(Ga, Mn)As Interfaces

F. Maccherozzi,<sup>1</sup> M. Sperl,<sup>2</sup> G. Panaccione,<sup>1</sup> J. Minár,<sup>3</sup> S. Polesya,<sup>3</sup> H. Ebert,<sup>3</sup> U. Wurstbauer,<sup>2</sup> M. Hochstrasser,<sup>4</sup>  
 G. Rossi,<sup>1,5</sup> G. Woltersdorf,<sup>2</sup> W. Wegscheider,<sup>2</sup> and C. H. Back<sup>2,\*</sup>

<sup>1</sup>Laboratorio Nazionale TASC, INFN-CNR, in Area Science Park, S.S. 14, Km 163.5, I-34012, Trieste, Italy

<sup>2</sup>Institut für Experimentelle Physik, University Regensburg, D-93040 Regensburg, Germany

<sup>3</sup>Laboratorium für Festkörperphysik, Wolfgang-Pauli-Strasse 16, ETH Hönggerberg, CH-8093 Zürich, Switzerland

<sup>4</sup>Dipartimento di Fisica, Università di Modena e Reggio Emilia, Via A. Campi 231/A, I-41100, Modena, Italy

<sup>5</sup>Department of Chemistry, Ludwig-Maximilians University Munich, Germany

(Received 15 January 2008; revised manuscript received 30 September 2008; published 22 December 2008)

We report x-ray magnetic circular dichroism and superconducting quantum interference device magnetometry experiments to study magnetic order and coupling in thin Fe/(Ga, Mn)As(100) films. We observe induced magnetic order in the (Ga, Mn)As layer that extends over more than 2 nm, even at room temperature. We find spectroscopic evidences of a hybridized *d* configuration of Mn atoms in Fe/(Ga, Mn)As, with negligible Mn diffusion and/or MnFe intermixing. We show by experiment as well as by theory that the magnetic moment of the Mn ions couples antiparallel to the moment of the Fe overlayer.

DOI: 10.1103/PhysRevLett.101.267201

PACS numbers: 75.50.Pp, 71.20.Nr, 78.70.Dm

Diluted magnetic semiconductors (DMS), in which magnetic impurities are artificially embedded into a semiconducting host, may allow the integration of the spin degree of freedom with semiconducting properties in a single material. Among the DMS, Ga<sub>1-x</sub>Mn<sub>x</sub>As with  $x \approx 1\%–10\%$  [(Ga, Mn)As] is a paradigmatic case: since the first synthesis by Ohno *et al.* [1], progress has been made both in the understanding of the carrier mediated mechanisms of the ferromagnetic (FM) state [2–4] and in the ability to raise the Curie temperature  $T_C$ , mainly by post-growth annealing [5]. To date, the possibility of spin-polarized current injection into (Ga, Mn)As, with all-semiconducting multilayers, has been demonstrated [6], but the highest  $T_C$  observed so far is  $\approx 170$  K, still well below room temperature. On the other hand, it is known that spin order may be induced in otherwise paramagnetic systems by FM proximity polarization [7], provided that the interface between the two materials is prepared in an adequate way. In our particular case, it is known that Fe grows epitaxially on top of the undoped counterpart of (Ga, Mn)As(001), namely, GaAs(001), without magnetically dead layers at the interface [8]. In this Letter we report experimental evidence of a robust magnetic coupling at the interface between (Ga, Mn)As and a thin FM Fe overlayer. In agreement with Monte Carlo simulations the effect persists until room temperature and extends over a (Ga, Mn)As region as thick as 2 nm due to proximity to the Fe overlayer. The comparison of x-ray absorption spectroscopy (XAS) and x-ray magnetic circular dichroism (XMCD) data obtained for Fe/(Ga, Mn)As(001) and Fe/GaAs(001), with Fe films grown in identical conditions, excludes significant Mn diffusion or segregation into the Fe films and gives spectroscopic evidence of a hybridized *d* configuration of the Mn atoms in the Fe/(Ga, Mn)As system, i.e., representative of Mn in a semiconducting environment. The Mn magnetization at the

interface is found to be aligned antiparallel with respect to the magnetization of Fe. Moreover, temperature dependent XMCD and SQUID measurements show that (i) Fe and Mn at the interface have a common magnetic behavior irrespective of the Mn concentration and (ii) the room temperature magnetization of (Ga, Mn)As is zero in the absence of the Fe overlayer. All these findings are in agreement with results of *ab initio* calculations performed for a Fe film on top of a (Ga, Mn)As(100) substrate.

XAS/XMCD experiments at the Fe- $L_{2,3}$  and Mn- $L_{2,3}$  absorption edges were performed in total electron yield mode at the APE beam line of the Elettra Synchrotron in Trieste. Ga<sub>1-x</sub>Mn<sub>x</sub>As films, with Mn concentration varying in the range of  $x = 0.02–0.06$ , have been grown by molecular beam epitaxy, and Fe thicknesses ranging from 0 to 4 nm have been investigated. Low energy electron diffraction, Auger spectroscopy, and core level x-ray photoemission spectroscopy have been used *in situ* to characterize the Fe/(Ga, Mn)As and Fe/Mn/GaAs(100) interfaces at different steps of the Fe growth. Similar results have been obtained on both polycrystalline Fe/(Ga, Mn)As and epitaxial Fe/(Ga, Mn)As(100) interfaces. Details of the experimental setup and of sample preparation and growth can be found in Ref. [9]. In a previous report we have verified that HCl etching produces Mn  $L_{2,3}$  XAS and XMCD spectra representative of the bulk (Ga, Mn)As free of Mn oxides [9–11] and mild Ar<sup>+</sup> sputtering (<2 min) at 750 eV efficiently removes the contaminated layer, but reduces the Mn magnetic signal [12].

Knowing that Mn doping in GaAs represents a highly nonequilibrium state, we followed the evolution of both XAS and XMCD line shapes of Mn intentionally grown on GaAs(100) in various chemical environments: namely, (i) a minute amount of Mn (0.02 nm) deposited on top of GaAs(100), (ii) the Mn/GaAs(100) interface of (i) covered by a Fe overlayer, (iii) a Mn thin layer sandwiched between Fe

films grown on GaAs(100) (i.e., a truly metallic environment), (iv) a  $\text{Fe}_{0.97}\text{Mn}_{0.03}/\text{GaAs}(001)$  alloy obtained by coevaporation. Results are presented in Fig. 1. Figure 1(a) shows Mn  $L_{2,3}$  spectra of a strongly oxidized (Ga, Mn)As as grown sample (Mn doping is 5%) (black curve), the same (Ga, Mn)As sample cleaned by mild sputtering (blue curve), and subsequently covered with 2 nm of Fe. We notice a close resemblance between the sputtered (Ga, Mn)As substrate and the Fe-covered one: both spectra show the hybrid  $d^4-d^5-d^6$  configuration of Mn in the GaAs matrix at the  $L_3$  edge, and the characteristic double broad peak structure at the  $L_2$  edge. This finding is in excellent

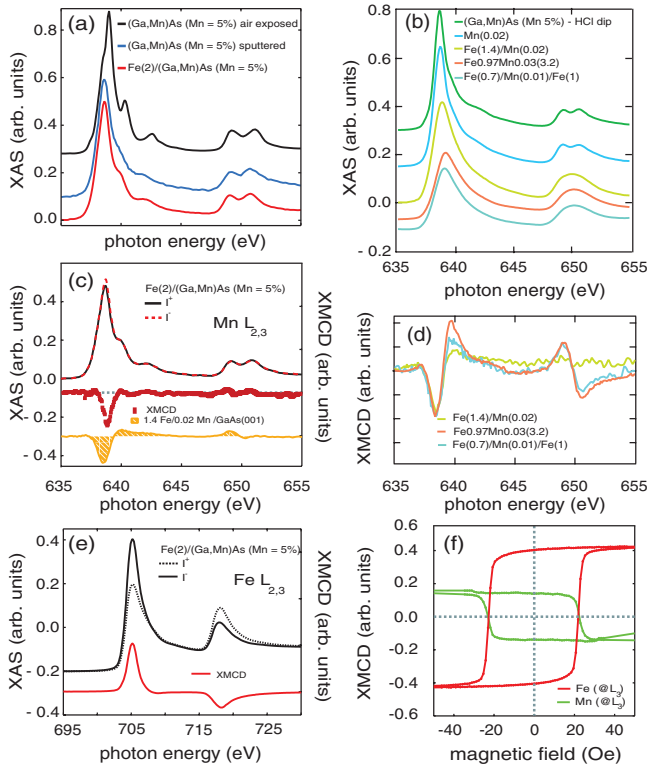


FIG. 1 (color). XAS/XMCD spectra measured in total electron yield at room temperature and at remanence. All thicknesses in the Figures are given in nanometers. (a) Mn  $L_{2,3}$  edges of (Ga, Mn)As (Mn 5%): as grown oxidized sample (black curve), after mild sputtering (blue curve), after Fe deposition (red curve). (b) Mn  $L_{2,3}$  edges of pure (Ga, Mn)As (Mn 5%) after HCl etching (green curve), 0.02 nm Mn/GaAs(001) (blue curve), 0.02 nm Mn/GaAs(001) with overgrowth of 1.4 nm Fe (yellow curve), 3.2 nm thick  $\text{Fe}_{0.97}\text{Mn}_{0.03}$  alloy grown on GaAs(100) (orange curve), 0.01 nm Mn sandwiched between two thin Fe layers grown onto GaAs(001) (turquoise curve). (c) Room temperature magnetization dependent XAS ( $I^-$ ,  $I^+$ ) and XMCD (red squares) spectra for the sample with 2 nm Fe/(Ga, Mn)As (Mn 5%). The yellow curve is the XMCD spectrum of 0.02 nm thick Mn/GaAs(001) film with 1.4 nm Fe overlayer. (d) Mn XMCD line shapes of different Mn samples corresponding to the spectra in (b). (e) XAS (black dots, black curve) and XMCD (red curve) spectra of 2 nm Fe/GaMnAs(Mn5%) at the Fe  $L_{2,3}$  edges. (f) Hysteresis curves measured at the maximum XMCD signal on Fe (red) and Mn (green).

agreement with previous results [9,10,13] and with both the reference (Ga, Mn)As spectrum obtained by HCl etching [green curve in panel 1(b)] and the spectrum of 0.02 nm Mn grown onto GaAs(100) [blue curve in 1(b)], thus indicating that Mn diluted in its semiconducting environment is not influenced by the growth of the Fe film. Conversely, if we cover the 0.02 nm Mn/GaAs(100) sample with a 1.4 nm Fe film the situation changes drastically [yellow curve in Fig. 1(b)]. One observes not only a clear broadening and small energy shift on the  $L_3$  edge but also, and more significantly, the disappearance of the double structure at the  $L_2$  edge. The same features are found in 1(b) for all spectra corresponding to Mn in a metallic environment, i.e., for a 3.2 nm thick  $\text{Fe}_{0.97}\text{Mn}_{0.03}$  alloy and for a 0.01 nm Mn layer sandwiched between two Fe layers grown onto GaAs(001) (orange curve and turquoise curve, respectively). Such differences are also reflected in the corresponding XMCD spectra of 1(c) and 1(d), in agreement with recent results [14]: the room temperature magnetization dependent ( $I^-$ ,  $I^+$ ) spectra for the sample 2 nm Fe/(Ga, Mn)As (Mn 5%) in 1(c) produces an XMCD spectrum (red squares) which is noticeably different from the XMCD spectrum of 1.4 nm Fe/0.02 nm Mn/GaAs(100) [yellow curve in 1(c)]. In contrast to the line shape obtained for Fe/GaMnAs, XMCD line shapes of different Mn samples display a positive feature at 640 eV, a plus and minus feature at the  $L_2$  edge, and a different energy position (150 meV) of the negative peak [1(d)]. Thus, the essential result is that there are clear spectroscopic evidences that Mn in the metallic Fe environment does not have the same electronic configuration as Mn in the GaAs host. Since all our Mn XAS and XMCD data for the system Fe/(Ga, Mn)As do show identical spectroscopic features as Mn in the GaAs host, we are able to exclude significant Mn diffusion or segregation into the Fe layer and/or a strongly intermixed Mn/Fe region.

The Fe and Mn  $L_{2,3}$  XMCD spectra recorded at room temperature for all Fe/(Ga, Mn)As (5% Mn, 0–4 nm Fe) samples show ferromagnetic order [Fig. 1(c), red squares, and Fig. 1(e), red curve], whereas Mn dichroism is absent in (Ga, Mn)As samples not covered by Fe. The dichroic signals are opposite in sign, indicating an antiparallel alignment between the Fe overlayer and the Mn in the DMS. Element specific XMCD hysteresis loops at both the Mn and the Fe  $L_3$  edges are presented in Fig. 1(f). A sizable Mn magnetic signal is found at remanence, with a coercive field identical to the one of Fe. Having ascertained that a direct proportionality is found between the Mn and Fe dichroic signals, we now address the ability of the Fe overlayer to induce magnetic order in (Ga, Mn)As. We define the percental XMCD, a quantity proportional to the magnetic moment, as  $D_{\text{Mn(Fe)}} = c \frac{I^+ - I^-}{I^+ + I^-}$ , where  $c$  is the correction for the partial circular polarization of the photons and the  $45^\circ$  angle of incidence. Figure 2(a) presents the evolution of the ratio  $r = \frac{D_{\text{Mn}}}{D_{\text{Fe}}}$  versus Fe thickness and temperature. For small Fe thicknesses,  $r$  depends

in first approximation linearly on both parameters. The values fall on a single curve with identical slope for a fixed temperature. In Fig. 2(b) we present the remanent XMCD signal of Fe and Mn as a function of temperature. The Fe XMCD signal does not decrease significantly, as expected for a 2 nm thick film, whereas one observes a decrease of the Mn magnetic signal. The Mn/Fe XMCD ratio decreases approximately linearly as a function of temperature. Extrapolation indicates that the magnetic coupling should be present well above room temperature. In Fig. 3 we show SQUID measurements of the spontaneous magnetization of (Ga, Mn)As (blue squares) and of Fe/(Ga, Mn)As (red circles) which was protected against oxidation by a Cu-capping layer immediately after the XAS/XMCD measurements. In the Fe/(Ga, Mn)As data, up to 60 K one observes the  $M(T)$  curve of bulk ferromagnetic (Ga, Mn)As offset by the Fe magnetization, similar to the one of the pure substrate (blue squares). For  $T > 60$  K the magnetization is entirely due to the Fe film, whose  $T_C$  is well above room temperature. The sample structure and its proposed magnetization profile at room temperature are schematically sketched in Fig. 3(b): the (Ga, Mn)As volume is divided in (i) the (Ga, Mn)As bulk region, (ii) the interface region with induced FM order, and (iii) the FM Fe overlayer. Based on the model sketched in Fig. 3(b) the magnitude of the Mn dichroism  $D_{\text{Mn}}$  can be described by

$\delta(x)dx$ , the dichroic signal which contributes at depth  $x$ . Assuming that the Mn concentration varies as  $\rho(x)$ , the measured intensity is attenuated by the exponential electron escape probability  $\exp^{-(x/\lambda_e)}$ , we obtain  $D_{\text{Mn}} = \int_0^\infty \delta(x)\rho(x)e^{-(x/\lambda_e)}dx / \int_0^\infty \rho(x)e^{-(x/\lambda_e)}dx$ . By assuming (i) a sharp interface, (ii) a uniform distribution of Mn in GaAs, and (iii) a steplike dichroism profile versus thickness  $\theta$ , we have  $\delta(x) = \delta_{\text{sat}}$  for  $\theta_{\text{Fe}} < x \leq \theta_{\text{min}}$ , and  $\delta(x) = 0$  elsewhere; we are now able to estimate a lower limit  $\theta_{\text{min}}$ , as the thickness of (Ga, Mn)As contributing to the FM signal at room temperature. Integration gives  $\theta_{\text{min}} = -\lambda_e \ln(\delta_{\text{exp}}/\delta_{\text{sat}})$ . We adopt the calculated value of  $\delta = \delta_{\text{sat}} = 59\%$  [15] and we consider the antiparallel layer of thickness  $\theta_{\text{min}}$  fully magnetized. In our experiment  $\lambda_e \approx 3$  nm and  $\theta_{\text{Fe}} = 4$  nm, then we obtain  $\theta_{\text{min}} = 2$  nm, corresponding to more than 7 monolayer (ML) of (Ga, Mn)As.

To support the interpretation of our experimental results we performed *ab initio* calculations for a Fe film (7 ML) on top of a (Ga, Mn)As substrate with 5% Mn (represented by a film of 14 ML). These calculations were done using the SPR-TB-KKR formalism [16] within the framework of the local spin density approximation [17]. Total energy calculations assuming parallel as well as antiparallel alignment at the (Ga, Mn)As/Fe interface identified the latter one to be energetically more favorable. The corresponding magnetization profile gives Fe moments close to that of pure Fe

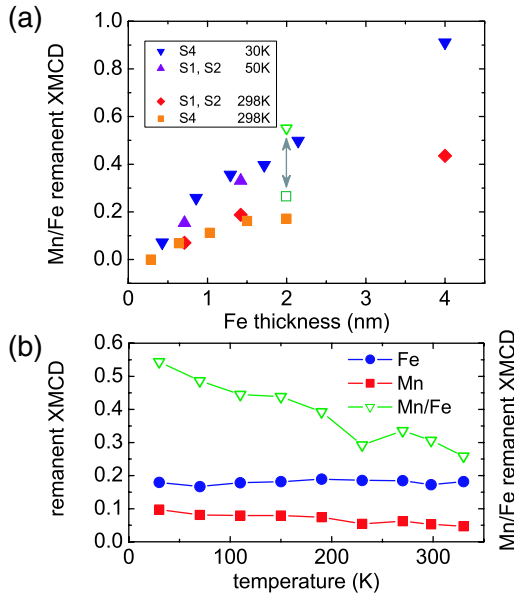


FIG. 2 (color online). (a) Ratio between Mn and Fe remanent XMCD signals in various samples as a function of Fe thickness (top) and temperature (bottom). Square symbols represent room temperature data, triangles represent low temperature data. All samples have a common temperature dependent slope as a function of Fe thickness. The Mn concentration ranges from S1 = 3%, S2 = 2% to S4 = 6%. The arrow indicates the temperature dependent measurements shown in (b). (b) Evolution of the Fe and Mn remanent XMCD signal and of their ratio as a function of temperature for a (Ga, Mn)As (Mn 5.5%) sample covered by a 2 nm thick Fe film.

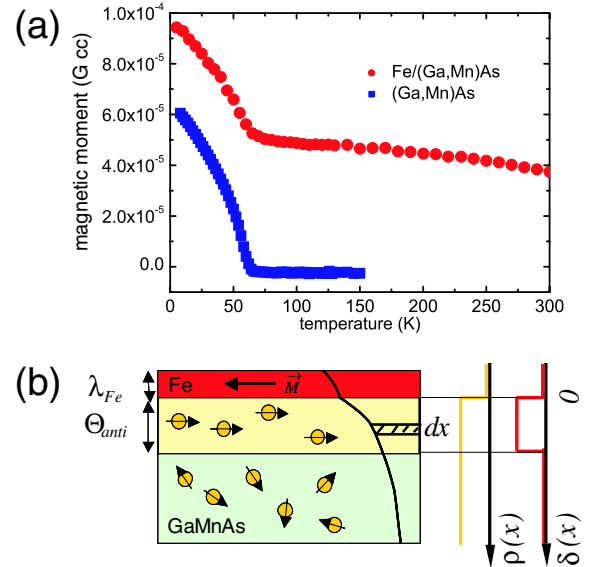


FIG. 3 (color online). (a) Spontaneous  $M(T)$  curves of sample 3 (6% Mn concentration) (red circles) and from a pure (Ga, Mn)As substrate (blue squares), measured during field cooling. Each point is determined by a linear extrapolation of  $M(H)$  ( $H = 0.475$ – $0.7$  kOe) to zero field. The field is high enough to saturate both the Fe and (Ga, Mn)As films. The Mn fraction located in the bulk is not affected by the surface and has the same  $T_C$  as the pure (Ga, Mn)As substrate (blue squares). (b) Sketch of a simple model for the Mn distribution  $\rho(x)$  and the fraction of ferromagnetic Mn at room temperature  $\delta(x)$  as discussed in the text.

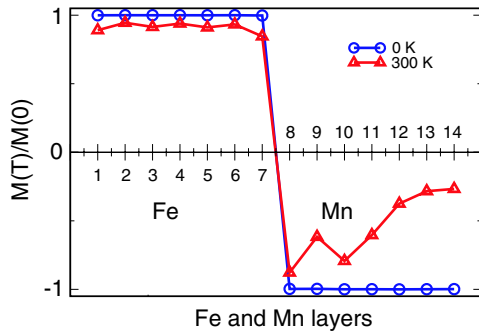


FIG. 4 (color online). Monte Carlo simulation of a Fe/(Ga, Mn)As film consisting of 7 ML of Fe and 7 ML of (Ga, Mn)As ( $x_{\text{Mn}} = 5\%$ ) compared to the calculation at  $T = 0$  K. A reduction of about 10% of the Fe moment is observed. The (Ga, Mn)As layer remains FM at room temperature and is coupled antiparallel to Fe.

( $2.1\mu_B$ ). In particular, at the interface there is hardly any change compared to the bulk Fe moment. On the (Ga, Mn)As side the Mn moment is close to  $4\mu_B$  with a reduction to about  $3\mu_B$  directly at the interface. The antiparallel coupling between Mn and Fe is also confirmed by calculations for the exchange coupling parameters  $J_{ij}$  [18]. Within the Fe layers the coupling is similar to bulk Fe with rather long-ranged dominantly FM coupling [19]. As found for bulk (Ga, Mn)As [20] the coupling is also dominantly FM within the DMS subsystem. However,  $J_{ij}$  drops very rapidly with the distance  $R_{ij}$  of atomic sites  $i$  and  $j$  leading to the relatively low  $T_C$  of pure (Ga, Mn)As [20]. The coupling of Fe and Mn moments close to the interface, however, is found to be strongly antiparallel. Although the coupling strength  $J_{ij}$  also decays fast with the corresponding distance  $R_{ij}$  one nevertheless can expect an appreciable induced magnetization of (Ga, Mn)As in the vicinity of the interface for temperatures well above its intrinsic  $T_C$ . This was indeed confirmed by Monte Carlo simulations. In the past this approach was applied, e.g., to pure Fe [21] as well as pure (Ga, Mn)As [20] giving  $T_C$  in good agreement with experiment. Figure 4 shows results for our Fe/(Ga, Mn)As model system. As one can see the strong exchange coupling within the Fe layer leads to a finite magnetization at  $T = 300$  K with the Fe moment reduced by 10% compared to its  $T = 0$  K value. For the (Ga, Mn)As subsystem the negative sign of  $M(T)/M(0)$  represents the antiparallel coupling to the Fe layer. The exchange coupling at the interface leads to average moments  $M(T)$  for the Mn atoms that are reduced to 70% of their value at  $T = 0$  K, up to the fourth atomic layer from the interface. With increasing distance from the interface the average magnetization of Mn layers decays but still has a finite nonvanishing value ( $\sim 25\%$ ) even for the 7th atomic layer. This further supports that the polarization induced by the Fe film extends indeed far into the (Ga, Mn)As.

In conclusion, we find spectroscopic evidences of a hybridized  $d$  configuration of Mn atoms, i.e., representative of Mn diluted in a semiconducting environment, in well characterized Fe/(Ga, Mn)As samples with minimal Mn diffusion or segregation. We observe antiparallel magnetic coupling between Fe and Mn, with FM order in the (Ga, Mn)As layer. The effect induced by the presence of the Fe overlayer, persists until room temperature, for various Mn concentrations and Fe thicknesses, and extends over a (Ga, Mn)As region as thick as 2 nm. Although further theoretical and experimental investigations are needed to fully control the proximity polarization effect, and to disentangle the role of substitutional versus interstitial Mn atoms on the magnetic properties in epitaxial samples, our findings suggest a pathway for the development of DMS-based devices with properly engineered FM interfaces.

Financial support by the DFG through the SFB 689 is gratefully acknowledged. This work has been partially funded by CNR-INFM. We thank M. Soda, J.C. Cezar, A. Verna, and G. Baraldi for support during the experiment.

\*christian.back@physik.uni-regensburg.de

- [1] H. Ohno *et al.*, Appl. Phys. Lett. **69**, 363 (1996).
- [2] A.H. MacDonald, P. Schiffer, and N. Samarth, Nature (London) **4**, 195 (2005).
- [3] T. Dietl, H. Ohno, and F. Matsukura, Phys. Rev. B **63**, 195205 (2001).
- [4] A. Kaminski and S. Das Sarma, Phys. Rev. Lett. **88**, 247202 (2002).
- [5] K. W. Edmonds *et al.*, Phys. Rev. Lett. **92**, 037201 (2004).
- [6] E. Johnston-Halperin *et al.*, Phys. Rev. B **65**, 041306 (2002).
- [7] J. Unguris *et al.*, Phys. Rev. Lett. **69**, 1125 (1992).
- [8] L. Giovanelli *et al.*, Phys. Rev. B **72**, 045221 (2005).
- [9] F. Maccherozzi *et al.*, Phys. Rev. B **74**, 104421 (2006).
- [10] K. W. Edmonds *et al.*, Appl. Phys. Lett. **84**, 4065 (2004).
- [11] K. W. Edmonds *et al.*, Phys. Rev. B **71**, 064418 (2005).
- [12] F. Maccherozzi *et al.*, Surf. Sci. **601**, 4283 (2007).
- [13] P. Gambardella *et al.*, Phys. Rev. B **72**, 045337 (2005).
- [14] Y. Takeda *et al.*, Phys. Rev. Lett. **100**, 247202 (2008).
- [15] H. Ohldag *et al.*, Appl. Phys. Lett. **76**, 2928 (2000).
- [16] H. Ebert and R. Zeller, SPR-TB-KKR package, <http://olymp.cup.uni-muenchen.de/ak/ebert/SPR-TB-KKR>, 2006.
- [17] S. H. Vosko, L. Wilk, and M. Nusair, Can. J. Phys. **58**, 1200 (1980).
- [18] A. I. Liechtenstein *et al.*, J. Magn. Magn. Mater. **67**, 65 (1987).
- [19] V. P. Antropov *et al.*, J. Magn. Magn. Mater. **200**, 148 (1999).
- [20] J. Kudrnovský *et al.*, J. Phys. Condens. Matter **16**, S5571 (2004).
- [21] V. Antropov, Phys. Rev. B **72**, 140406 (2005).